



PSEUDO-DYNAMIC TESTING OF A FULL-SCALE RCS FRAME: PART 2 – ANALYSIS AND DESIGN IMPLICATIONS

Paul CORDOVA¹, Greg DEIERLEIN², Chui-Hsin CHEN³, Wen-Chi LAI³, Keh-Chyuan TSAI⁴

SUMMARY

This is the second of a two-part paper, describing an investigation of a full-scale three-story composite steel-concrete moment frame, which was pseudo-dynamically loaded to simulate its earthquake performance out to story drift ratios of 5.5%. The frame was subsequently tested under a monotonic push out to an interstory drift of 10%. This paper summarizes the analytical studies of the test frame, including comparisons with measured response and design implications. Damage indices are investigated to help interpret the analytical results and relate the calculated engineering demand parameters to physical damage in the frame. In terms of peak displacements and overall response, the analytical and measured frame response agree fairly well up to drift ratios of about 3%. Beyond this, discrepancies occur, which are likely due to degradation effects (e.g., local flange buckling) that are not modeled in the analysis. Comparison between calculated damage indices and observed damage suggest the need for further research to improve the performance simulation tools.

INTRODUCTION

This is the second of a two-part paper describing a pseudo-dynamic test of a full-scale three-story three-bay composite steel concrete frame, conducted through international collaboration between researchers in Taiwan and the United States. The frame consists of reinforced concrete columns and steel (composite) beams and was tested at the National Center for Research on Earthquake Engineering (NCREE) in Taiwan. Background on RCS frames and details of the test specimen design, construction, and test results are summarized in the companion paper by Chen et al. [1]. This paper focuses on the validation of simulation models and the resulting design implications.

Being the largest and most realistic composite frame ever tested in a laboratory, the test provides a unique data set to validate both computer simulation models and seismic design provisions for RCS frames. This paper begins with a brief overview of some of the key design issues that influence the overall frame behavior. Following this is a discussion of the analytical models used to simulate the test through inelastic

¹ Res. Asst., Blume Earthquake Engr. Center, Stanford Univ., Stanford, CA; cordova@stanford.edu

² Professor & Director, Blume Earthquake Engr. Center, Stanford Univ., e-mail: ggd@stanford.edu

³ Research Assistant, National Center for Research in Earthquake Eng., Taipei, Taiwan, email: chchen@ncree.gov.tw, r90521215@ms90.ntu.edu.tw

⁴ Professor, Dept. of Civil Eng., National Taiwan University, Taiwan, e-mail: kctsai@ce.ntu.edu.tw

time history analyses. These were conducted with a computational platform called OpenSees (Open System for Earthquake Engineering Simulation [2]), developed through the Pacific Earthquake Engineering Research (PEER) Center, and PISA2D [3], developed by researchers at NCEE. Simulation results are compared to the measured frame response for earthquake ground motions corresponding to earthquake hazard levels of 50%, 10% and 2% chance of exceedence in 50 years. The analytical and test results are processed through damage indices and related to the actual physical damage within the frame. Finally, conclusions are drawn regarding model accuracy, overall performance prediction, and seismic design implications from the test frame.

TEST FRAME

As summarized in the companion paper by Chen et al. [1], the test frame is based on a three-story building designed according to the International Building Code (IBC) [4] and related standards as a ductile moment frame for a three-story office building located in a high seismic region. The reader should refer to the companion paper for details of the frame geometry, member sizes, etc. What follows is a summary of the key design parameters and their impact on the seismic performance of the frame.

Key Design Issues

SCWB: The strong-column weak-beam (SCWB) criterion quite often controls the column sizes in ductile (special) moment frames. The IBC [4] and ACI-318 [5] provisions require that the ratio of nominal column to beam strengths should be greater than 1.2, except at the top floor beams where SCWB criterion is not required. Since the intent of the test program was to examine the limits of current code provisions, we took a liberal interpretation of the SCWB criterion with respect to whether the calculation is made using properties of the steel or composite beam for the SCWB check. Differences can be significant, since the difference in nominal strengths between the steel and composite beam assumption is about 30%. The calculated nominal strength ratios, based on the steel beam strengths, all equal or exceed the specified ratio of 1.2. However, as shown in Fig. 1a, when calculated based on composite beam strengths, several of the joints (highlighted by dashed boxes) fall below the minimum value of 1.2. Some ratios even indicate that the composite beam strength exceeds the column strengths (values less than 1.0). The values shown in Fig. 1a are based on the assumption that beams flexed in positive bending will act compositely and those in negative bending will act as steel beams. Figure 1b summarizes results of the same checks using measured, as opposed to nominal, material strengths of the beams and columns. Being as the main intent of the SCWB criterion is to avoid story mechanisms, the fact that one joint in a story violates the criterion is not necessarily detrimental to the frame behavior. For example, one might interpret the values for the first and second floors in Fig. 1b as meeting the intent of the SCWB criterion, since the average ratio for a story exceeds 1.2. As will be discussed later, the SCWB ratios alone do not provide an accurate gage of where inelastic deformations will occur under earthquakes.

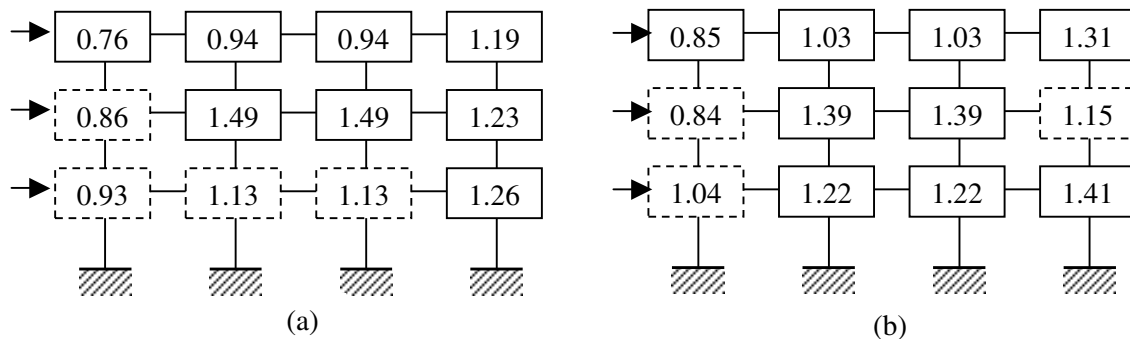


Figure 1 – $\Sigma M_c / \Sigma M_g$ ratios at each joint assuming composite beams with (a) nominal properties and (c) measured properties.

Beam and Column Splices: The steel beams are spliced 1500 mm away from the face of the column. This location is a compromise between competing desires to minimize the offset for ease of construction (fabrication and shipping of the precast column-beam assemblies) and maximizing the offset so as to reduce the design moment for the splice. Following the requirements for steel moment frames in FEMA 350 [6], the bolted splice connection is proportioned with a minimum design strength equal to 1.2 times the probable moment at the column face, calculated as $M_{pr} = C_{pr} R F_y Z = (1.2)(1.1) F_y Z$. Further, in accordance with US construction practice and the AISC Seismic Provisions [7], the connection is proportioned based on bearing strength of the bolts, as opposed to slip critical values. As reported in the companion paper, this design philosophy resulted in slipping of the bolts during all of the pseudo-dynamic tests. The main consequence of the slipping was loud bolt banging during the test; otherwise, the bolt slippage did not have any appreciable effect on the overall frame behavior.

Precast column splices are located 1-meter above the foundation footing and directly above the connection band plates (at the top of slab) at floors one and two. The splice at the base of the 1st floor column was raised above the footing, since this location is known to experience large hinge rotations. The influence of the splice location on performance at the column base was examined through subassembly tests, conducted prior to the frame study. Two splice locations were investigated in these tests – one being flush against the column-footing interface and the second being 1-meter up the height of the column. Both tests showed that the precast connection could develop and maintain the full column strength through large inelastic deformations, although the specimen with the splice adjacent to the footing displayed more pinching behavior. In the end, due to the critical nature of this region, it was decided to place the splice at the 1-meter location. The splice location for 2nd and 3rd floor columns is less critical because analysis studies have shown that severe column hinging is not likely to occur above the floor beam – except in instances where the SCWB criterion is not met and a severe story mechanism could occur. Since it is common practice in Japan to splice the column right above the floor, and since the intent of the frame test was to investigate the limits of performance relative to standard practice, it was decided to locate the splices directly above the beam-column joints.

Shear Studs in Hinge Region: FEMA 350 [6] does not permit the placement of shear studs within the expected plastic beam hinge region, which is assumed to extend from the column face to one-half beam depth away from the column. The concern is that the shear studs will lead to strain localization and premature beam flange fracture during plastic hinging. During construction of the test frame, the workers inadvertently placed shear studs within the hinge region of the 2nd and 3rd-floor beams. This construction mistake was noted at the time, but it was decided against trying to remove the studs due to concerns about damaging the beam flange. As it turned out, the studs in these regions did not cause a problem, although before drawing general conclusions from this, it will be important to consider the level of inelastic deformations sustained by these hinges.

Recap of Testing Program

The testing program utilizes a pseudo-dynamic loading methodology to simulate earthquakes on the test structure. Based on information from pre-test analyses, conducted using PISA2D and OpenSees (presented later in this paper), two earthquake records were chosen among strong motion recordings collected during recent earthquakes. The two selected records are TCU082-EW (from the 1999 Chi-Chi earthquake) and LP89G04-NS (from the 1989 Loma Prieta earthquake), both of which are considered to represent general motions without near-field directivity effects. The original test plan was to scale these two records in acceleration amplitude to represent four separate pseudo-dynamic loading events, which were sequenced as follows: (1) TCU082 scaled to represent a 50/50 hazard intensity, i.e., with a 50% chance of exceeding in 50 years, (2) LP89G04 scaled to a 10/50 hazard, which represents the design basis

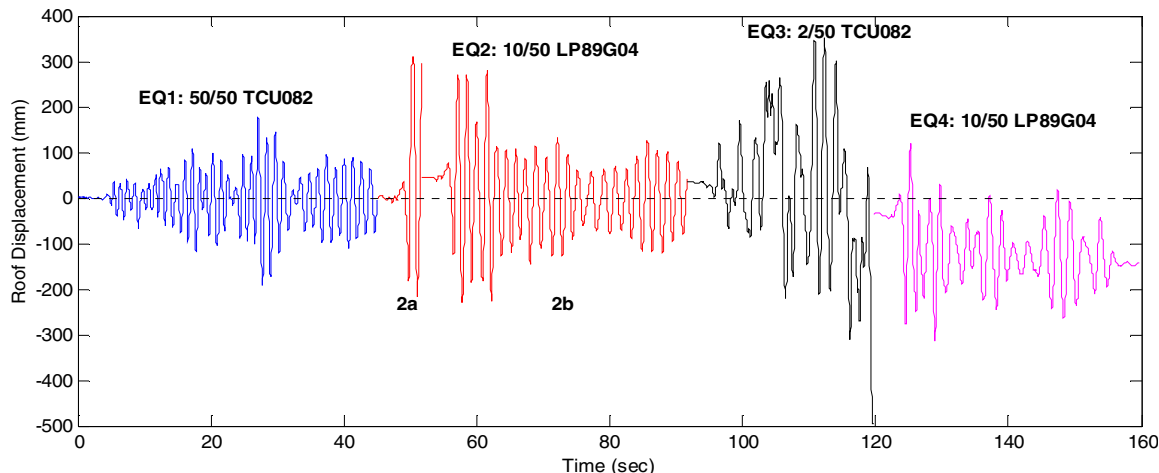


Figure 2 – Time history of roof displacements during sequence of pseudo-dynamic loading events

earthquake, (3) TCU082 scaled to a 2/50 hazard, which represents the maximum considered earthquake, and (4) LP89G04 scaled to a 10/50 hazard – identical to loading (2). The record scaling is based on matching their spectral acceleration at the first mode frame period to the specified earthquake hazard levels. After the pseudo-dynamic tests, a final monotonic pushover load (using the IBC 2000 [4] loading pattern) is applied to a maximum roof drift ratio of 8 percent.

Shown in Fig. 2 is the measured roof time history from the pseudo-dynamic tests. It turned out that some unexpected events during testing led to modifications in the planned loading protocol. Specifically, the initial 10/50 loading was interrupted due to a problem with the lateral frame bracing (point 2a in Fig. 2), which created some out of plane deformation and hinging at the column bases. Following repair of the bracing, the 10/50 record was re-run at 80% of its original intensity (point 2b in Fig. 2). This was done because the frame had already experienced several large loading excursions prior to the interruption in the 10/50 test, such that re-running the record at full scale would over-damage the structure. The second unexpected event occurred during the 2/50 record, when the frame deflected more than expected and the actuators exhausted their 500 mm stroke capacity at about 28 seconds into the 2/50 record (corresponding to the 120 second point in the cumulative plot of Fig. 2). As the frame had experienced all the major loading excursions up to this point, the decision was made to discontinue the 2/50 test at this point. Finally, since the 2/50 loading introduced permanent displacements that reduced the available stroke capacity for subsequent tests, the frame was partially straightened using the actuators after the 2/50 event. Further details on the testing and observed damage are given in the companion paper [1].

OPENSEES MODELS

Extensive analytical studies were performed on the frame specimen both prior to and after the actual test. These studies serve two main purposes. First, results of these analyses were important to help plan the test, specifically to make decisions regarding record selection so as to help ensure that the actuator stroke and story shear capacity are not exceeded during the test. Secondly, once the test is completed, comparisons of measured and analysis results provide data to validate the structural analysis models. The analyses described in this paper were all conducted using OpenSees [2] - an object-oriented simulation framework developed by researchers in the PEER Center for simulating the seismic response of structural and geotechnical systems (see <http://opensees.berkeley.edu>). OpenSees is an open source program and is continually evolving as researchers improve existing and add new components. Presented within this section is a description of the analytical model of the frame and the results that lead to the selection of the records and the final configuration of the actuators.

Fiber Section Flexibility-Based Beam-Column Elements

The RC columns and composite beams are modeled in OpenSees by flexibility-based, beam-column fiber elements. The flexibility-based elements are derived from exact force interpolation functions and therefore do not encounter a discretization error, as is generally found in the stiffness-based elements [8]. This allows for the columns and beams to be each modeled as a single element, and therefore reduce the overall computation time.

Fiber sections consist of steel, confined concrete, and unconfined concrete uniaxial material models. The steel material model [9] is a basic model that incorporates isotropic strain hardening, while the concrete material model [10] represents the concrete crushing and residual strength in compression and tensile strength with linear strain softening. The frame model presented within this paper utilizes the measured material properties of steel beams, reinforcing bars, and column and slab concrete. The Scott/Park/Priestley [11] model is used to modify the concrete's strength parameters to account for the amount of confinement provided by the reinforcing hoops.

To ensure the validity of these fiber section elements, they have been calibrated to the NCREE subassembly experiments and numerous other tests within the literature. Figure 3a shows the results from a composite beam subassembly test [12] compared with the OpenSees model. In the frame model, it is assumed that the effective slab width for composite action is equal to the column width. Presented in Fig. 3b are the results of a RC column subassembly tested in NCREE [13] compared with the OpenSees fiber element model. The results from the simulation demonstrate that OpenSees is able to capture the overall behavior of these elements quite well.

Finite-Size Inelastic Beam-Column Joint Model

The composite joints are represented with an OpenSees joint element that models the finite size and joint kinematics. Joint panel shear in RCS joints is governed by very fat hysteretic loops and modeled with the steel material model used in the fiber sections. The joint bearing deformations are related to concrete crushing and gap openings above and below the steel beam. This behavior exhibits pinching and is modeled using a hysteretic material model. The joint model and the two nonlinear springs have been calibrated to subassembly joint tests performed by Kanno [14]. Joint stiffness and strength parameters for both failure mechanisms are defined by equations developed by Kanno and Deierlein [15].

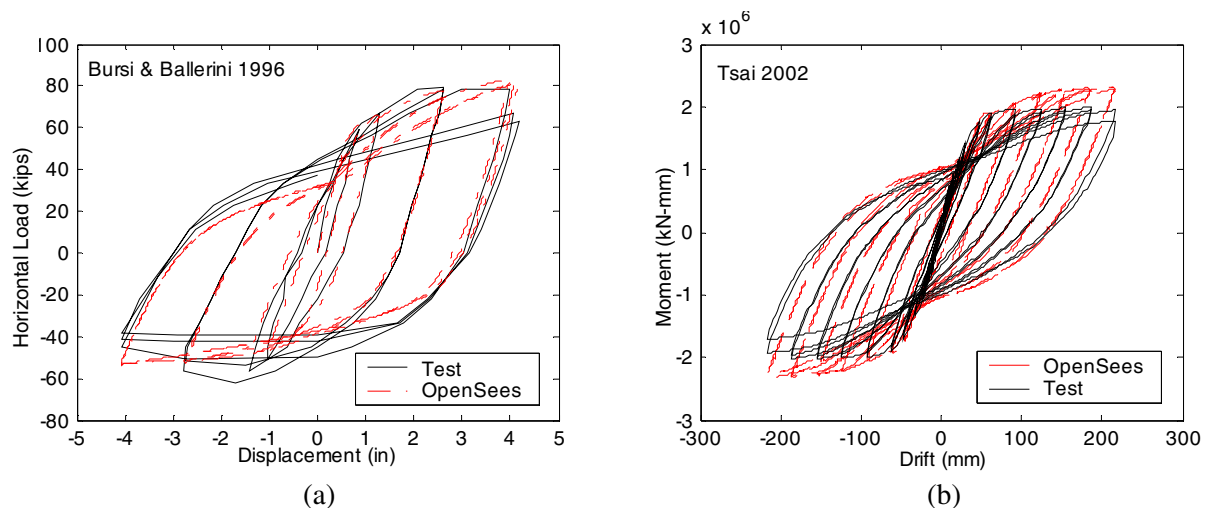


Figure 3 – Validation of fiber section flexibility-based elements, (a) composite beam, (b) RC column.

Test Frame Model

The test frame is one of two frames assumed to provide lateral resistance for a theoretical three-story building with a plan area of 1,176 square meters per floor. In the test and analytical model, the seismic mass is based on one-half of the dead load of the entire building, which is about four times larger than the tributary gravity load on the frame. A leaning column is included in the analysis and pseudo-dynamic models to account for the P-Delta effects induced by the seismic mass. The load on this leaning column is based on recommendations from FEMA 356 [16] by the following equation, $1.1D+0.275L$, where D and L are the service dead and live loads. Since the direct gravity load tributary to the frame is small relative to other effects, and since applying the tributary load to the test frame would complicate the loading apparatus, the gravity load from the tributary width of this frame is simulated by simply adding it into the leaning column.

As previously discussed, the test frame is subjected to a sequence of records scaled to various hazard levels. The damage that is incurred by the frame is not repaired between each event (i.e. concrete cracking, yielding, local buckling, permanent drift, etc.). Therefore, the OpenSees model is set up to account for the progressive accumulated damage from the sequential loading events applied in the test.

Another consideration in developing the frame model relates to modeling rotation at the column bases associated with yield penetration and bond slip in the concrete footing. This will lead to a reduction in the overall frame stiffness and less concentrated damage in the column base hinges as compared to a fixed base model. To capture this effect, concentrated rotational elastic springs are inserted between the first-story columns and column bases. These springs are assigned elastic stiffness equal to the rotational stiffness of the column, which essentially doubles the flexibility of the first-story columns. This model is based on findings within the literature that claim that bond slip accounts for nearly 50% of flexural deformations in experiments on fixed-fixed reinforced concrete beam columns. This base spring is also included and validated in the RC column calibration study shown above in Fig. 3b.

A key aspect of the frame behavior that is not captured by the analytical model is strength and stiffness degradation of the steel beam hinges due to local flange buckling. The fiber section element assumes plane sections remain plane and cannot easily pick up such behavior. It will be shown later that this effect is indeed an important one, and provides additional flexibility to the beams in the large excursions of the test frame. This suggests the need for future research and development to incorporate this effect.

ANALYTICAL VERSUS EXPERIMENTAL RESULTS

Using the OpenSees model described in the previous section, the pseudo-dynamic frame response was simulated under the prescribed ground motions. This includes the truncated records and the realignment push that occurred after the 2/50 event. The only difference between the test and the dynamic analysis model is that the analysis model necessitated the introduction of zero amplitude regions between events to damp out transient vibrations.

Global Response

The initial stiffness the OpenSees model matches quite well with that of the test frame, with both resulting in a natural fundamental period of approximately 1 second. Preliminary elastic events were simulated to ensure that the pseudo-dynamic algorithm and the actuators were working properly. The test results from these events compared quite well with the analytical results, which assured that the test frame and the laboratory equipment were functioning as expected and that the testing program could proceed.

Samples of the recorded test results versus the analytical results are shown in Figs. 4 and 5 for the 50/50 and 2/50 Chi-Chi event, respectively. For the 50/50 level earthquake, the time history of the roof displacement (Fig. 4a) compares with the analytical results rather well up until approximately 25 seconds, where one can begin to see the phase shift between the two. This is a result of some softening within the test frame that is not picked up by the analytical model. The maximum and minimum interstory displacements and the story shear comparisons are shown in Figs. 4b and 4c, respectively. Differences between the model and the test frame maximum displacements range from 2% to 30%, while differences in story shears range from 3% to 10%.

Prior to the 2/50 level event, the structure has already been subjected to two major events (the 50/50 and the 10/50) and has experience cyclic component damage as well as some residual drift. The observed residual drift of the test frame is different than what OpenSees predicts, which makes it difficult to compare the subsequent transient response because of the permanent shift in the entire history. In order to properly compare the results, the residual drifts have been removed from each of the plots in Fig. 5, i.e. all histories begin at zero displacement. The roof displacement time history (Fig. 5a) shows that there has definitely been a shift in the period of the test frame that is not being captured by the OpenSees model. This implies that the stiffness degradation within the analytical models is not properly picking up what is happening in the test. It should also be noted, that severe local beam flange buckles occur during about 18

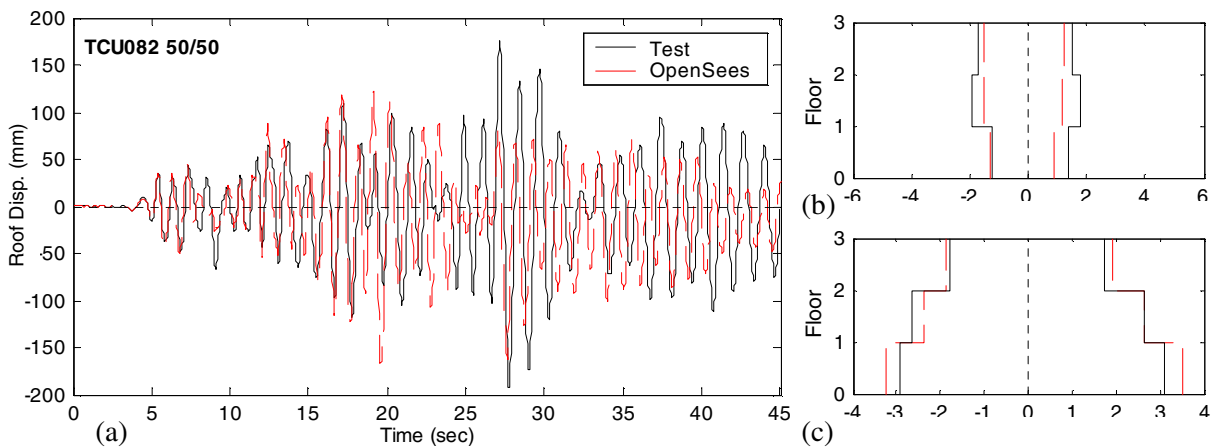


Figure 4 – EQ#1, TCU082 50/50: Measured versus analytical response of (a) roof displacement, (b) max/min IDR, and (c) max/min actuator force.

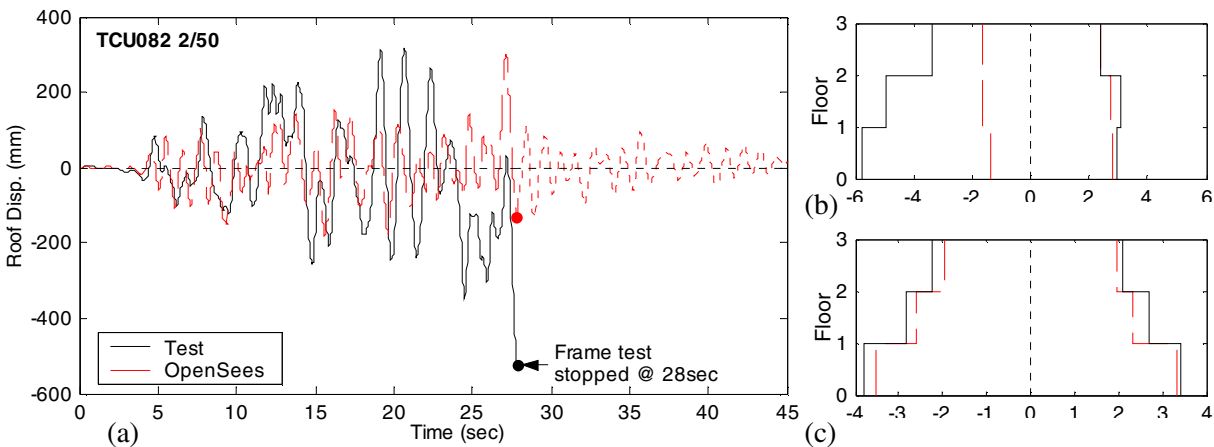


Figure 5 – EQ#3, TCU082 2/50: Measured versus analytical response of (a) roof displacement, (b) max/min IDR, and (c) max/min actuator force.

seconds into the record, which cannot be modeled by the fiber section element. This additional flexibility in the test frame is evident in the much larger interstory drifts observed during this event (Fig. 5b) and the much larger excursions after 20 seconds into the record. The excursion at approximately 24 seconds is not picked up by the analytical model and permanently offsets the two responses. Differences between the model and the test frame's maximum displacements range from 2% to 73%, while the agreement in story shears is much better, with a range from 4% to 16% between the measured and calculated values. Fig. 5a also shows the OpenSees results through the end of the 45 second earthquake. From this it can be seen that the excursion at 28 seconds was indeed the maximum pulse of the record, and beyond this point, all other cycles were smaller and less significant to the overall behavior of the frame.

Not shown here are results for the maximum displacements for the 10/50 design level earthquake (LP89G04), which were predicted within a range of 2% to 30%. The story forces were predicted with an error that ranges between 3% and 50%.

Local Response

Over three hundred data channels were recorded during the test, with a large majority of these dedicated to tracking the local response of the beams, slabs, joints, and columns. A small sample of these is presented here, including the force versus rotation plots of the hinge regions of a first floor exterior beam and an interior first floor column base. Note that the internal element forces from the test are not measured directly, and given the indeterminacy of the frame, their computation required assumptions from the OpenSees model on the column shear distributions and member inflection points.

For the 50/50 event, both the beam (Fig. 6a) and the column (Fig. 7a) experience slight nonlinearities that are adequately captured by the OpenSees models. The plots show that the stiffness of the elements is also picked up quite well. The 2/50 event produces the largest excursions of all the earthquake events, with beam rotations reaching nearly seven times that of the 50/50 event and column rotations up to five times. The 2/50 beam response (Fig. 6b) from the OpenSees model is not as representative of the real response as one would hope, which is largely due to the fact that the analysis is not picking up the local buckling that is occurring in the negative cycles. The last negative cycle, which reaches nearly 0.07 radians (70 milli-radians), corresponds to the maximum negative excursion shown in Fig. 6a near 28 seconds. This provides insight as to how important it is to model the stiffness degradation due to local buckling, and it explains why the OpenSees model is failing to pick up these large excursions in the test frame. The analytical model is also underestimating the positive composite strength of the beam, which suggests that the effective slab width should be increased. The 2/50 column response (Fig. 7b) is slightly more representative than the beam response, but the bond slip and overall stiffness degradation in the test is not correctly being modeled.

DAMAGE INDICES

In this section, the OpenSees results are interpreted through local damage indices and related to the physical damage and performance limit states in the frame. These limit states are referred to as specific damage designations used in FEMA 356 [16] and similar standards, such as immediate occupancy, life safety, and collapse prevention. Immediate occupancy corresponds to the onset of structural damage while collapse prevention is the point in which the structural system is becoming unstable. Life safety is an intermediate level that accepts a certain level of damage to structural and non-structural elements, but ensures the general safety of the occupants. While system damage descriptions of this sort are helpful to describe acceptance criteria and performance targets, the authors also recognize that more explicit and detailed models are currently under development by PEER and other organizations.

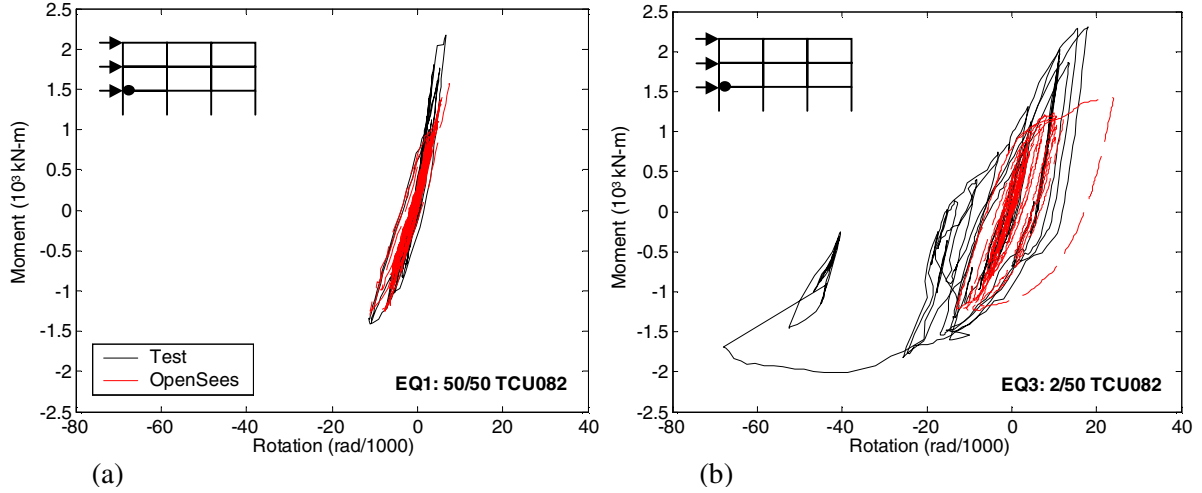


Figure 6 – Local response for exterior 1st-floor beam for (a) 50/50 and (b) 2/50 TCU082 event.

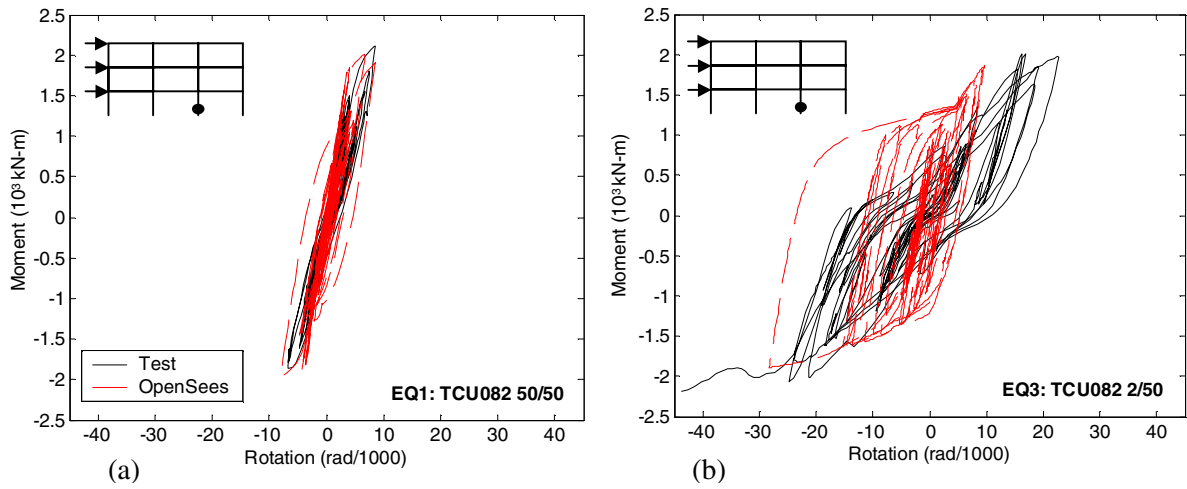


Figure 7 – Local response for interior 1st-floor column for (a) 50/50 and (b) 2/50 TCU082 event.

Damage Model

The local damage index presented herein is based on the work of Mehanny and Deierlein [17]. Chief characteristics of this index are to (1) account for cumulative damage, (2) reflect the temporal effects of loading sequence, and (3) readily accommodate the response of structural components with unsymmetrical behavior, e.g., composite beams. The index is described by the following expression,

$$D_{\theta}^+ = \frac{(\theta_p^+ I_{\text{current PHC}})^{\alpha} + \left(\sum_{i=1}^{n^+} \theta_p^+ I_{\text{FHC},i} \right)^{\beta}}{((\theta_f - \theta_y)^+)^{\alpha} + \left(\sum_{i=1}^{n^+} \theta_p^+ I_{\text{FHC},i} \right)^{\beta}} \quad (1)$$

where inelastic component deformations (expressed symbolically as θ) are distinguished between primary and follower cycles and accumulated over the loading history. A Primary Half Cycle (PHC) is a half cycle with an amplitude that exceeds that in all previous cycles, and the Follower Half Cycles (FHC) are all the preceding and subsequent cycles of smaller amplitude, including the previously eclipsed PHCs. The denominator term $(\theta_f - \theta_y)^+$ is the plastic rotation capacity of the element under monotonic loading in the

positive deformation direction, and α , and β are calibration parameters. A similar damage component D_{θ}^{-} is defined for negative deformations. The positive and negative indices are then combined into a single damage index as follows, $D_{\theta} = \sqrt[\gamma]{(D_{\theta}^{+})^{\gamma} + (D_{\theta}^{-})^{\gamma}}$, where γ is a third calibration parameter. Component failure is defined when $D_{\theta} \geq 1.0$. The following default parameters are recommended for RC columns and composite beams: $\alpha = 1.0$, $\beta = 1.5$ and $\gamma = 6.0$ parameters. For composite joints, the recommended values are $\alpha = 0.75$, $\beta = 3.0$, and $\gamma = 5.0$. See Mehanny and Deierlein [17] for further discussion on this damage index as well as the definition of the plastic rotation capacity.

This damage index can be roughly distinguished into four divisions that correlate to the damage state of the element. For values less than 0.3, it is assumed that there is very little damage to the element and corresponds to the immediate occupancy structural performance level. For values between 0.3 and 0.6, the structural element is assumed to experience noticeable damage, such as spalling of cover concrete and minor shear cracking in RC columns, and hinging and some local buckles in steel beams. In terms of the component damage and necessary repairs, this region of the damage index roughly corresponds to a life safety limit state. Between 0.6 and 0.95, the structural element is assumed to be a near collapse state, with extensive cracking and hinge formation in RC columns and significant hinging and local buckles for the steel beams. Beyond 0.95, it is assumed that the capacity of the element is lost. How well these suggested indices relate to the observed frame damage is examined in the next section.

Global View

Using the plastic rotation output from the OpenSees model, component damage indices for all members and joints in the frame are calculated for the entire loading protocol. The results of this process are summarized in Fig. 8 for damage occurring during the 50/50 and 2/50 TCU082 events. For clarity, values below $D_{\theta} = 0.3$ (30%) are not shown in these figures. Recall that the observed damage state of the frame after the 50/50 earthquake is limited to minor concrete cracking and steel beam yielding, requiring little if any repair. The D_{θ} -values for many elements are less than 30 – 40% (Fig. 8a), which is consistent with the observed damage. However, there are several members that reach higher damage values, which are not consistent with the observed damage. In particular, the interior base columns each have a D_{θ} -value of 52%, which suggests that we should at least see some cover spalling and maybe shear cracking, neither of which physically occurred in the members. The exterior beams in the first and second floors have a D_{θ} -value of approximately 50%, while the third floor beam reaches values up to 72%. Again, this damage

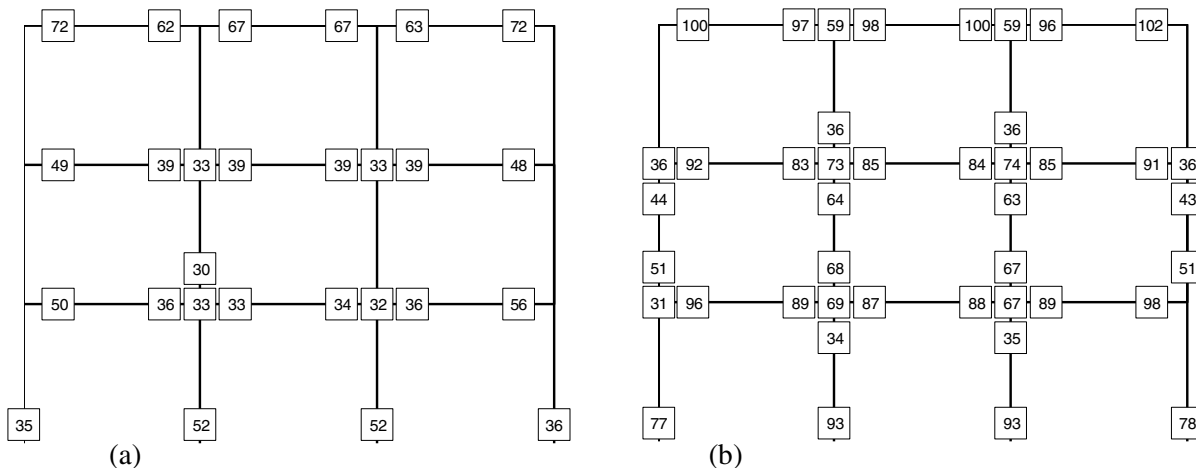


Figure 8 – D_{θ} -value (%) for the beams, columns, and joints after the
(a) 50/50 and (b) 2/50 TCU082 event.

index suggests that these beams will experience hinging and some local buckles. In the test frame there was no local buckling of any of the steel beams and only very slight yielding during this event, which was only noticed due to minor flaking of the paint in the hinge zones.

After the 2/50 event, researchers present at the frame test concluded that the frame had reached the collapse prevention limit state, characterized by significant local damage (concrete crushing, large crack openings, local beam flange and web buckling) and residual drift that were on the verge of being technically infeasible to repair. Figure 8b definitely reflects that there is severe damage to the frame after this event, with all of the beams reaching D_{θ} -values between 85 and 102% and the base columns within the 77-93% range. This seems to be an accurate representation, because at this point, the base columns experienced extensive hinging, with distributed cracks and spalling of the cover concrete and the beams in the first and third floors had been subjected to extensive yielding and significant local buckles of the bottom flange. However, the OpenSees model overestimates the amount of inelasticity occurring in the second floor beam. Whereas the calculated damage indices are between 83% and 93%, this beam only experienced slight yielding with no local buckles. The OpenSees model correctly picks up damage (concrete cracking and spalling) that concentrates in the upper region of the second floor columns, with damage indices reaching up to 64%. Several of the interior joints in the model are showing a D_{θ} -value of up to 74%, which is not representative of the observed damage, which was limited to slight cracking.

Local View

Here we will focus in more detail on the evolution of calculated indices and physical damage of the interior base column (1C3) and exterior 1st floor beam (1B1S). The plot in Fig. 9 shows the evolution of the D_{θ} -values for the 1C3 and 1B1S elements over the four earthquake time histories. Also included is the damage evolution during two time intervals, marked I and II, which stand for (I) the first 7 seconds of the LP89G04 event (1a) that had to be stopped and (II) the frame straightening imposed after the 2/50 event. The damage calculations in Fig. 9 are based on input data from both the OpenSees analysis and from the measured (tiltmeter) response of column 1C3 and beam 1B1S. Comparison of the analytical and measured response data is presented to help determine whether discrepancies between the damage index, D_{θ} , and the observed physical damage are inherent to the damage index or are a by-product of differences in the input response data (i.e., plastic rotations) used to calculate the index. Note that the tilmeter data was not recorded during the realignment push (event II), which explains the break in the plots for the test data during this segment.

During the 50/50 event, the progression of the column damage index based on OpenSees is consistent with the index based on the measured data, although the final values on the order of $D_{\theta}=0.4$ to 0.5 are high relative to the minor amount of physical damage that occurred to the column during this loading. Contrary to the column response, the OpenSees value of D_{θ} for the beam diverged from the value based on measured data after approximately 20 seconds into the record. This divergence is inconsistent with beam hinge rotation data shown in Fig. 6a, which indicates that the OpenSees response matches the test response quite well, suggesting that the D_{θ} -values should be similar to one another. Also, the final value of $D_{\theta}=0.5$, calculated by OpenSees, is inconsistent with the minor observed damage to the beam. The most probable explanation for this difference is that perhaps some of the assumptions used in extracting the plastic deformation from the tilmeter response are not valid during this event.

These general trends continue through the first design-level event (LP89G04 1b), where OpenSees predicts that both the column and beam have D_{θ} -values equal to approximately 0.8 at the end of the test, versus values of $D_{\theta}=0.9$ for the column and $D_{\theta}=0.6$ for the beam, based on measured data. Photos of the physical damage to this beam and column, shown in Figs. 10a and 10c, reveal that the damage in these members was relatively minor. This is in contrast to the predicted damage indices, which incorrectly

suggest that both elements would have experienced severe hinging representative of a near collapse limit state. Thus, in this instance, damage values based on both the OpenSees and measured data, significantly overestimate the expected damage to these elements.

If we examine these elements again after the 2/50 event, we can see that all of the D_{θ} -values are near 90%, which would indicate that these elements have lost most of their capacity. During the final cycle of this event, the D_{θ} -value of the test beam surpasses the OpenSees prediction (see Fig. 6b). This dramatic jump is a result of the large flange and web buckles (Fig. 10b) that occurred during this cycle, which is not picked up in the analytical model. The concrete column also shows well developed hinging with large cracks and minor spalling (Fig. 10d). Granted that these elements are experiencing some significant damage, but to estimate that they are at a near collapse state may not be accurate, especially considering that another successful design earthquake and a final pushover of the frame were completed after this event.

In general, these results show that while OpenSees is able to capture the evolution of the plastic deformation response of the column base, there are significant differences in results from the analytical and test beam damage index. By closer examination of Fig. 9, one can see that a majority of the error arises from the divergence in the first 50/50 event. After this event, when comparing the analytical and test results, it seems that all of the excursions are captured since the general shape of the curve and the change in the D_{θ} -value is consistent between the two. Another major jump arises at the end of the 2/50 event when the beam exhibits significant local buckles, which is again not captured in the OpenSees model. This suggests why the frame model was not able to capture some of the large excursions that occurred during the 2/50 event. Both the analytical and test D_{θ} -values consistently overestimate the damage for this column and beam, suggesting that either the calibration coefficients should be adjusted or that the levels for the damage states should be reevaluated.

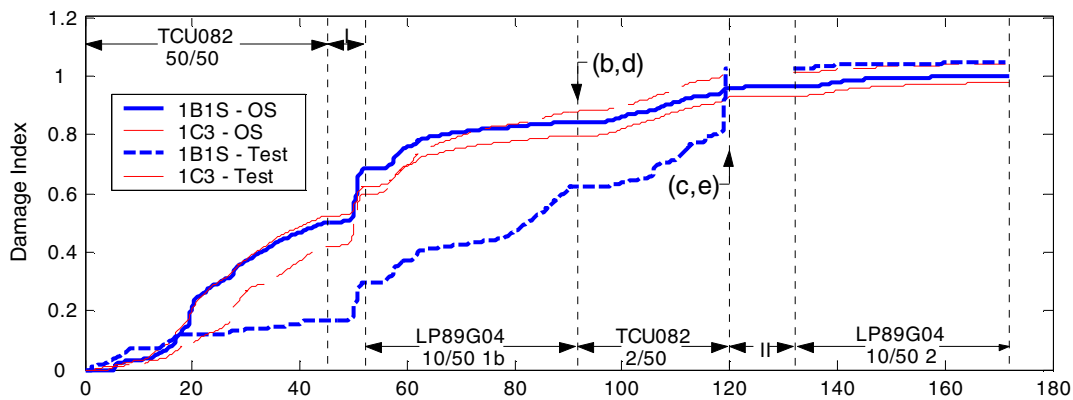


Figure 9 – Damage index progression for interior base column and exterior 1st-floor beam.

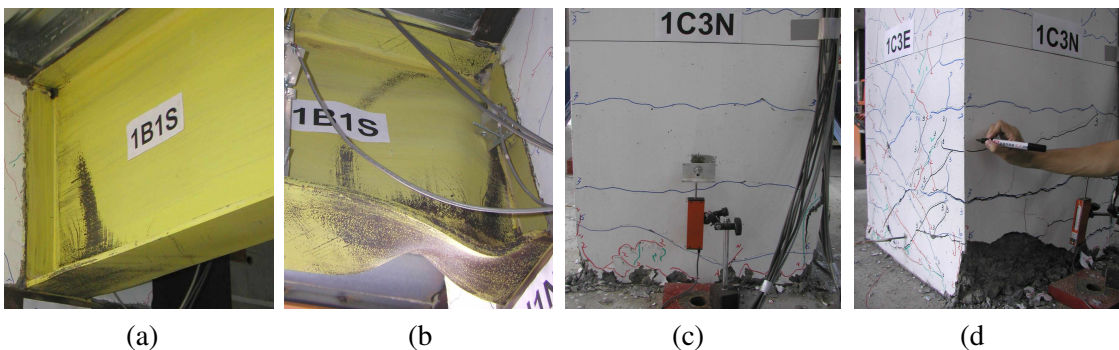


Figure 10 – Physical damage in beam (a,b) and column (c,d) after the 10/50 design level earthquake and 2/50 maximum considered earthquake, respectively.

CLOSING COMMENTS AND OBSERVATIONS

Even when designed to test the limits of current building code provisions, the RCS test frame showed excellent seismic behavior under various seismic hazards. The damage incurred by the frame after each event correlates well with the performance targets of immediate occupancy, life safety, and collapse prevention, implied by building code provisions. The SCWB issue proved to be important to the final deformation mechanism in the frame, though the calculated SCWB indices are not a good indicator of the observed performance. In the 2/50 event, we began to see the story deformations concentrate in the lower two stories, with the second floor beams experiencing only minor yielding while some cracking and minor spalling occurred in the upper region of the second floor columns. This type of behavior became more pronounced during the final pushover. Examining the SCWB ratios in Fig. 1b, one can see that interior joints of the second floor have the highest ratios in the entire frame (1.39), yet hinging still formed in the columns just below the joints. These test results imply that the current version of SCWB may not be adequate to prevent hinging from occurring in the columns. The SEAOC Seismology Committee has drafted a proposed Blue Book [18] provision change for the SCWB criterion, which recommends a comparison between the strength of the beams and that of the columns below the beam (i.e., rather than the columns above and below the beam). The test data tend to support this new provision, since the second floor columns (where hinging occurred) do not meet the proposed requirement, whereas all the other floors do.

The performance of the slab and the composite action in the beams is much better than what was initially expected based on subassembly tests, which exhibited quick deterioration of the slab and the shear studs that ultimately leads to loss of composite strength. In the frame test, the integrity of the slab, the shear studs, and the composite action of the beams was maintained throughout the entire loading protocol. Moreover, the shear studs within the hinging region did not lead to any fracture problems in the steel beams. The composite joints, including the third floor joints, performed exceptionally well throughout all phases of the loading protocol. With the standard details, these joints were strong enough to force hinging within the composite beams. This is similar to the findings in previous research [14] and the subassembly tests performed at NCREC.

Although there was some initial concern on the location and durability of the precast column connections, these connections ultimately performed very well and prove to be a viable connection method for the seismic design of RCS frames. The beam splices did experience some slight yielding during the series of earthquakes, and were ultimately the controlling failure mechanism during the final pushover tests when the splices ultimately failed in ductile fracture. This raises some concerns, considering that the design intent is to ensure that beam yielding occurs before premature failure of the beam splice. On the other hand, this is happening at extreme deformations and may be deemed okay.

The OpenSees analytical models conducted for this study were shown to capture behavior of the subassembly tests quite well; and the models captured the test frame behavior fairly well under the 50/50 and 10/50 events – out to interstory drifts of about 3%. Large differences between the analytical and test frame behavior occurred during the larger excursions in the 2/50 event, which appear due to the fact that the OpenSees model did not model the large local buckles that occurred in some of the beams (see Fig. 10b). It was also observed that the stiffness of the test frame softened much more than that of the analytical model, partly due to the local buckling, but also as a result of the stiffness degradation of the concrete columns and the bond slip that occurred at the base. These differences are apparent when one examines the local behavior of the test frame compared with the analytical behavior in the latter stages of the 2/50 record and the subsequent 10/50 record. Nevertheless, the initial 50/50 and 10/50 events were predicted with errors in displacements that range from 2% to 30% and errors in shear from 3% to 50%. This error could possibly be reduced if one models the local buckles and the stiffness degradation better.

On the other hand, one must keep in mind that even though the test frame was quite elaborate, it still is only a highly idealized representation of real buildings. Thus, how well these models can accurately simulate the response of real buildings is still uncertain.

The OpenSees frame model combined with the Mehanny damage index allows us to predict and compare the damage in the analytical model to the test frame. It was shown that this worked fairly well in predicting the ultimate capacity of a member, but it seemed that in the progression of the damage throughout the history it overestimated the damage in the earlier stages. It may be possible to correct this by the re-calibrating the recommended α , β , and γ coefficients, which will be pursued by the authors in future studies. However, one is still faced with the underlying limitation of the simulated demand parameters under extreme loadings.

ACKNOWLEDGEMENTS

The authors gratefully acknowledge support to plan and conduct the full-scale composite frame test from the National Science Council (NSC91-2711-3-319-200-14) and the National Center for Research in Earthquake Engineering (NCREE) of Taiwan. Additional support for planning and analyzing the test was provided by the National Science Foundation (Award Number CMS – 9975501) and the Pacific Earthquake Engineering Research Center (Award Number EEC-9701568). Also acknowledged are the management, research and technical staff at NCREE and the Ruentex Construction and Development Company. Any opinions, findings, or other conclusion or recommendations expressed in this material are those of the authors and do not necessarily reflect those of the sponsors and contributors.

REFERENCES

1. Chen, C.H., Lai, W.C., Cordova, P., Deierlein, G.G., Tsai, K.C. (2004), "Pseudo-dynamic test of full-scale RCS frame: Part I – Design, Construction, and Testing" *Proceedings of 13th World Conference on Earthquake Engineering*, Paper #2178, Vancouver, Aug. 2004.
2. McKenna, F., and G. L. Fenves (1999), "G3 Class Interface Specification Version 0.1 – Preliminary Draft," Pacific Earthquake Engineering Research Center, University of California at Berkeley, USA
3. Tsai, K.C., Chang, L.C., "The Platform and Visualization of Inelastic Structural Analysis of 2D Systems PISA2D and VISA2D," Report No. CEER/R90-08, Center for Earthquake Engineering Research, National Taiwan University. (in Chinese), 2001.
4. IBC 2000 (2000), "International Building Code," *Inter. Code Council*, Falls Church, VA, April 2000.
5. ACI (2002), *Building Code Requirements for Structural Concrete*, ACI-318-02, American Concrete Institute, Farmington Hills, MI.
6. FEMA-350 (2000), "Recommended Seismic Design Criteria for New Steel Moment-Frame Buildings," SAC Joint Venture (funded by Federal Emergency Management Agency), June 2000
7. AISC (2002), *Seismic Provisions for Structural Steel Buildings*, American Inst. of Steel Construction, Chicago, IL
8. Neuenhofer, A. and Filippou, F.C. (1997), "Evaluation of Nonlinear Frame Finite Element Models", *Journal of Structural Engineering*, American Society of Civil Engineers, Vol. 123, No. 7, July 1997, pp. 958-966
9. Filippou F.C., Popov E.P. and Bertero V.V. (1983), "Modeling of R/C joints under cyclic excitations," *Journal of Structural Engineering*, Vol. 109, No. 11, pp. 2666-2684.
10. Park, R., Kent, D. C. and Sampson, R. A. (1972), "Reinforced Concrete Members with Cyclic Loading," *Journal of the Structural Division*, ASCE, 98, ST7, July 1972, pages 1341-1360, Proc. Paper 9011
11. Scott, B.D., Park, R., and Priestley, M.J.N. (1987), "Stress-Strain Behavior of Concrete Confined by Overlapping Hoops at Low and High Strain Rates," *ACI Journal*, Jan-Feb 1982, pp. 13-27

12. Bursi, O. S., Ballerini, M. (1996), "Behavior of a steel-concrete composite substructure with full and partial shear connection," Eleventh World Conference on Earthquake Engineering [Proceedings], Paper No. 771
13. Tsai, K.C. and Chen, P.C. (2002), A Study of RC Column-to-Foundation and Steel Beam-to-RC Column Joints for an RCS Frame Specimen, Technical Report, National Center for Research on Earthquake Engineering. (in Chinese)
14. Kanno, R. (1993), "Strength, Deformation, and Seismic Resistance of Joints between Steel Beams and Reinforced Concrete Columns," Ph.D. Thesis, Cornell University, Ithaca, NY.
15. Kanno, R. and Deierlein, G.G. (2002), "Design Model of Joints for RCS Frames," Composite Const. in Steel and Concrete IV, ASCE, pp. 947-958.
16. FEMA-356 (2000), "Prestandard and Commentary for the Seismic Rehabilitation of Buildings," ASCE (funded by Federal Emergency Management Agency), Reston, Virginia, November 2000
17. Mehanny, S.S.F., Deierlein, G.G. (2001), "Seismic Damage Analysis – Assessing Collapse Prevention for Composite Moment Frames," JSE, ASCE 127 (9) pg. 1045-1053.
18. SEAOC (2003), "Recommended Modifications to Building Code Requirements for Reinforced Concrete," *SEAOC Blue Book*, Article No. 20090-03, in publishing.